Ceramics

A novel fabrication technique of toughened TiC-based solid solution cermets using mechanochemical synthesis

Xiao Chen[1] ⬤, Zhenhua Yao[2], Weihao Xiong[3], and Jianfeng Xu[1],*

[1] State Key Laboratory of Digital Manufacturing Equipment & Technology, School of Mechanical Science and Engineering, Huazhong University of Science and Technology, Wuhan 430074, People's Republic of China

[2] School of Materials Science and Engineering, Wuhan University of Technology, Wuhan 430070, People's Republic of China

[3] State Key Laboratory of Material Processing and Die & Mould Technology, School of Materials Science and Engineering, Huazhong University of Science and Technology, Wuhan 430074, People's Republic of China

ABSTRACT

Ceramic–metal composite powders (Ti,M)C-Ni (M = Mo, W and Ta) were prepared from elemental powders using a one-step mechanochemical synthesis method through high-energy ball milling. The microstructure and mechanical properties of the resulting cermets were also investigated. The analytical results revealed that ball milling of Ti-M-C-Ni elemental powders triggered a combustion reaction between Ti and C. The reaction resembled a fast sintering process which facilitated alloy elements atoms dissolve into the newly formed TiC, synthesizing the (Ti,M)C-Ni composite powders. The microstructure of the sintered (Ti,M)C-Ni cermets consisted of the core-rim structure grains and homogenous grains. High-resolution transmission electron microscope analysis results revealed that there was a misorientation between the ceramic phase and the binder phase in the cermets, but the interface between the core and the rim was coherent. The cermets exhibited mechanical properties that were comparable to conventionally produced cermets, particularly in fracture toughness which was as high as 12.45 MPa m$^{1/2}$. The excellent cohesion between the Ni binder and the (Ti,M)C solid solution and the reduction in the interfacial stress in ceramic grains were believed to be responsible for the enhanced toughening of the cermets.

Address correspondence to E-mail: jfxu@hust.edu.cn

Introduction

TiC/Ti(C,N)-based cermets are promising material to replace WC–Co cemented carbide for high-speed cutting and metallic hot forming tools due to the lower cost and excellent properties which include high melting point and hardness, improved thermal conductivity, oxidation resistance, creep resistance and a low friction coefficient with metals [1–5]. Typically, the cermets consist of TiC/Ti(C,N) ceramic grains embedded in a Ni and/or Co alloys which act as the binder. A variety of secondary carbides such as Mo_2C/Mo, WC and TaC/NbC are used to improve the specific properties of TiC/Ti(C,N)-based cermet, such as sinterability, hot hardness and thermal shock resistance [6–9]. These additives also resulted in producing typical core–rim ceramic grains in the cermets. The core of the grains is undissolved TiC/Ti(C,N) particles and the rim is (Ti,Me)C/(Ti,Me)(C,N) solid solution (Me = Mo, W, Ta, Nb, etc.) [10–16]. In general, the rim phase can be divided into two regions, an inner rim close to the core–rim boundary which is richer in heavy metals and an outer rim close to the rim-binder phase boundary with less heavy metal content than the inner rim [10–16].

Although TiC/Ti(C,N)-based cermets have many advantages over WC-based cemented carbide, including hot hardness, thermal conductivity, oxidation resistance, creep resistance [3–6], the cermets exhibits lower fracture toughness than the cemented carbide, which limits the cermets' industrial applications. The inferior fracture toughness of the cermet is attributed to both the poor wettability of liquid Ni on TiC/Ti(C,N) and to a large quantity of highly strained core-rim interfaces in the ceramic grains [4, 17, 18]. The use of pre-alloyed single-phase and homogeneous solid-solutions such as (Ti,W)C, (Ti,W)(C,N) as the hard phase has been proven to be effective for improving the toughness of cermets [17–20]. However, the aforementioned carbides or carbonitride solid solutions are generally prepared using a carbothermal reduction method, which is time-consuming and requires a high-temperature vacuum furnace and other expensive instruments [21].

Recently, mechanochemical processing has been used as a powerful manufacturing technique for the synthesis of several novel powder materials [22–27] and offers advantages over other methods such as low cost, small particle sizes and narrow size distribution [27]. Researchers have reported that carbonitrides solid solutions such as (Ti,Nb)(C,N), (Ti,Ta)(C,N) and (Ti,Nb,Ta)(C,N) were synthesized by mechanochemical processing under high-pressure nitrogen atmosphere [24–26]. Nevertheless, as a kind of inert gas, nitrogen was difficult to be captured during the mechanochemical process due to the instantaneous high temperature. As a result, the acquired solid solutions deviated their designed ingredients significantly and the metals powders remained, which caused the generation of intermetallics during the mechanochemical reactions and the subsequent sintering process and deteriorated the mechanical properties of cermets.

The element N in Ti(C,N)-based cermets system plays a role of refining the grain size and improving the mechanical properties [8]. However, in view of the difficulty of the capture of N from the nitrogen atmosphere by the mechanochemical method, other approaches should be sought to refine grain size and avoid a potential generation of intermetallics. On the other hand, only a small amounts of Ta and Nb are usually added in the cermets system in order to improve the hot hardness and thermal shock resistance [6, 7]. Instead, W and Mo are the most important and commonly used alloy elements for eliminating pores and refining grain size [5, 10, 17]. To date, however, there are few researches concerning the mechanochemical synthesis of carbides solid solutions that contain W or Mo, which are essential elements for improving the performance of the cermets. Besides, the cermets prepared by the mechanochemical method did not exhibit acceptable mechanical properties due to the existence of intermetallics in the binder phase [24–26]. Thus, there are many issues need to explore concerning the preparation of superior cermets by means of the mechanochemical method. In this reported work, three types of cermets (Ti,W)C-Ni, (Ti,Mo)C-Ni and (Ti,Ta)C-Ni were prepared from elemental powders using a mechanochemical processing combined with the pressureless sintering, and the synthesis process of the composite powders, mechanical properties and microstructures of the cermets were also investigated.

Experimental procedures

Commercial Ti powder (purity 99%, particle size 45 μm, oxygen content 0.25 wt%), Mo powder (purity 99.9%, particle size 2.80 μm, oxygen content 0.25 wt%), W powder (purity 99.9%, particle size 3.80 μm, oxygen content 0.15 wt%), Ta powder (purity 99.5%, particle size 38 μm, oxygen content 0.18 wt%), Ni powder (purity 99.8%, particle size 2.25 μm, oxygen content 0.14 wt%) and graphite powder (purity 99.9%, particle size 5.50 μm) were used in this study. Table 1 lists the nominal composition of the four raw powder mixtures, they are labeled P1–P4, respectively. P1 is a comparison among these four samples.

The synthesis procedure consisted of placing mixtures and WC–Co balls with diameter of 8 mm into stainless steel vials which were then filled with highly pure argon (99.999%). The outer diameter, inner diameter and height of the stainless steel vials are 130 mm, 100 mm and 150 mm, respectively. The powder mixtures with the weight of 50 g for every system were then planetary ball-milled with a ball-to-powder weight ratio of 30:1 and a rotation speed of 400 rpm. During milling, the external temperature of the vial was monitored using an infrared thermometer (F62Max, Fluke, China). As the temperature abruptly increased by 60 °C, the MSR was ignited. After ignition, the milling process was continued to reach four hours so that homogenous products were obtained. The phases of milled products were identified using XRD (XRD-7000, Shimadzu, Japan). The powder specimens milled with different durations for XRD are obtained by uninterrupted ball milling. The morphology of the milled powders was examined using SEM (Nova Nano 450 and Quanta 200, FEI, USA) equipped with an EDS (EDAX, USA).

In order to improve the powder yield, the composite powders were obtained by several minutes of wet ball milling using alcohol. The slurry was then sieved by 325 mesh and dried in a vacuum oven. All of the dry powders were broken and then sieved by 200 mesh without the addition of forming agent. The synthesized composite powders were compacted in a rectangular mold with a uniaxial pressure of 300 MPa and then sintered at 1445 °C under vacuum (10^{-3}–10^{-2} Pa) for 1 h. The sintered specimens were grinded by diamond wheels using a machine tool to remove the surface scale before the mechanical properties tests. The transverse rupture strength (TRS) of the cermets was determined using a universal material testing machine (Zwick/Roell Z020, Germany) employing the three-point bending method (span 14.5 mm, strain rate was 0.5 mm/min). The dimension of the rectangular bar specimen was 20.00 mm × 6.50 mm × 5.00 mm. The TRS values were averaged for five specimens.

After the TRS tests, the fractured surfaces of the specimens were grinded to flat and then polished by different grades of diamond abrasive papers and diamond pastes to mirror surfaces for XRD analysis and SEM observation. The interfacial structure of the cermets was observed using FTEM (Tecnai G2 F30, FEI, USA). The TEM samples were prepared by a Focused Ion Beam (FIB, FEI Helios NanoLabG3 CX). A protective platinum with the thickness of 1 μm was deposited on the surface before digging out the piece by FIB. The ion beam with the voltage of 30 kV and the current of 2.5–9.3 nA was used in the digging process. Then the voltage of 30 kV and the current of 0.79 nA was used in the rough thinning process, and the voltage of 2–5 kV and the current of 23–41 pA was used in the fine thinning process.

Porosity of the polished specimens was evaluated using ISO 4505. The hardness was measured by a Vickers hardness tester (432 SVD, Wolpert Wilson Instrument, China) with an indenter load of 30 kg over 15 s, and fracture toughness (K_{IC}) was calculated from the crack lengths caused by the indentations using the expression derived by Shetty et al. [28].

Table 1 Starting composition, ignition time and characters of the synthesized powders

Sample	Target composition	Ignition time (min)	Ceramic phase	Lattice constant (nm)
P1	TiC-20 wt% Ni	98	TiC	0.43265
P2	$(Ti,W_{0.05})C$-20 wt% Ni	106	(Ti,W)C	0.43239
P3	$(Ti,Mo_{0.1})C$-20 wt% Ni	107	(Ti,Mo)C	0.43207
P4	$(Ti,Ta_{0.05})C$-20 wt% Ni	86	(Ti,Ta)C	0.43311

Results

Synthesis of the composite powders

An abrupt increase in temperature of the milling vials was observed in each system after milling for a while, which indicated that a mechanically induced self-sustaining reaction (MSR) occurred in these four mixtures. The MSR appeared to be instantaneous as is the case in the self-propagating high-temperature synthesis (SHS) process. The average ignition time, i.e., activation period, for each system is shown in Table 1 and it was reproducible within ± 3 min. Figure 1 shows XRD patterns of P1–P4 after milling for different durations. The phase composition of the products consisted mainly of a TiC/TiC-type phase and Ni. This was attributed to the high adiabatic

temperature of TiC (T_{ad} = 3210 K [27]), which caused an occurrence of the self-sustained reaction (P4 also contained some TaC due to its high adiabatic temperature 2700 K [27]). The XRD data were used to estimate the lattice parameters of the carbide phases using the Nelson–Riley extrapolation function [29] and the results are provided in Table 1. By comparing the lattice parameters of the TiC and TiC-type phase, it is reasonable to conclude that the TiC-type phases in P2, P3 and P4 were (Ti,W)C, (Ti,Mo)C and (Ti,Ta)C solid solutions, respectively. However, some Mo, W and Ta powders were residual in the systems after MSR from the XRD patterns, which indicated that complete solid solutions had not resulted. As the milling time was prolonged, W and Ta remained in the mixture system, but Mo disappeared. Meanwhile, the diffraction peaks of WC abrasives from the
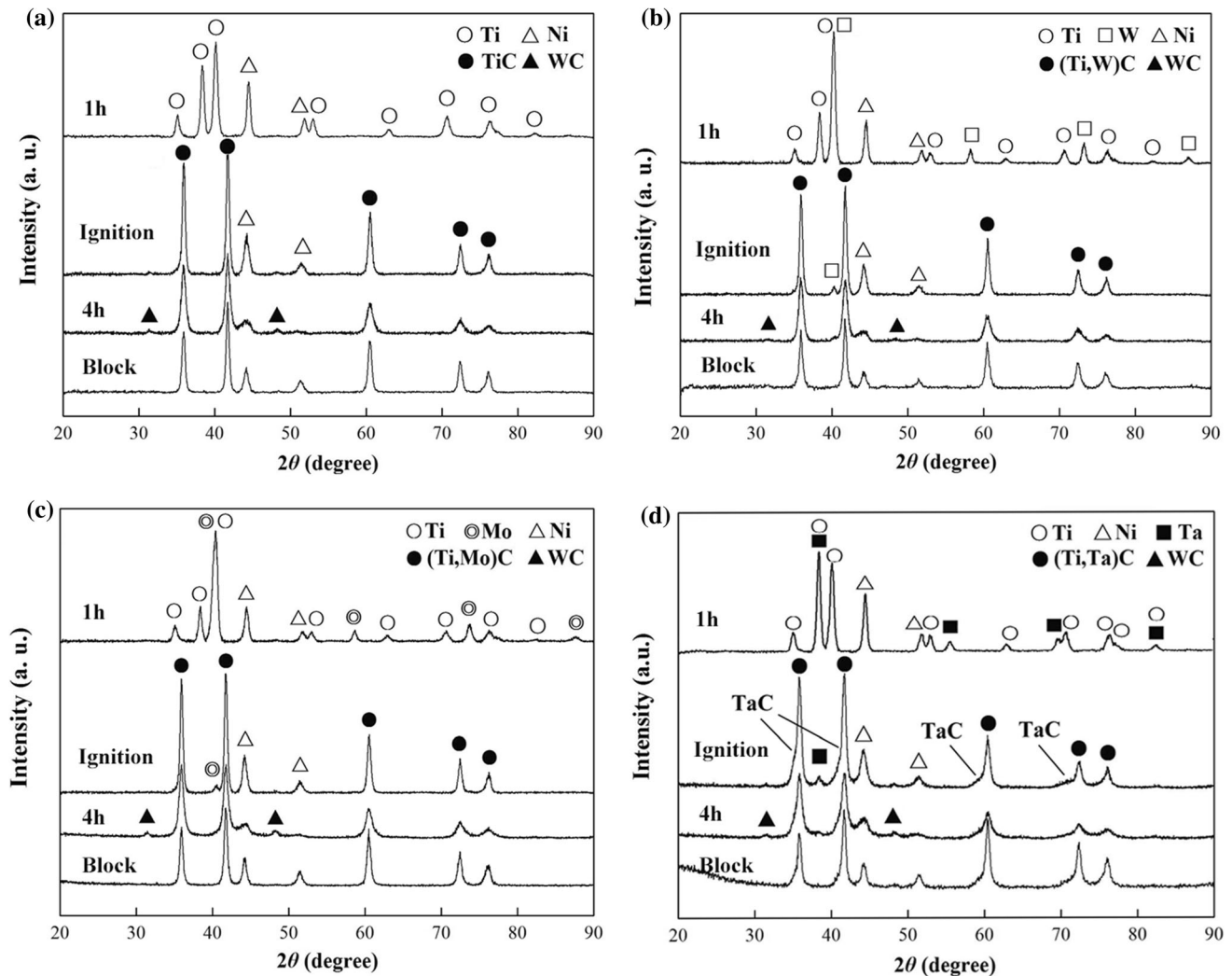

Figure 1 XRD patterns of the mixtures after milling for various times: **a** Ti-C-Ni; **b** Ti–W-C-Ni; **c** Ti-Mo-C-Ni; **d** Ti-Ta-C-Ni.

milling balls were observed in the XRD patterns. The morphology of the resulting composite powders is shown in Fig. 2a.

Besides the ultrafine composite powders, it also can be found some irregular porous blocks as shown in Fig. 2c with the size of 1–15 mm in the four mixtures after the MSR was ignited. These blocks had a phase composition similar to the composite powders (Fig. 1). The surface of the block is full of pores in which an abundance of smooth spherical ceramic particles can be observed. From the microstructure of the block shown in Fig. 3, the spherical ceramic grains were distributed uniformly in Ni binder phase. However, there was a difference in the

ceramic grain microstructures between the Ti-C-Ni system and the Ti-M-C-Ni systems (M = W, Mo, and Ta, hereinafter inclusive). The former only exhibited homogenous TiC grains while the latter exhibited a core-rim structure grains, as shown in Fig. 3b–d. The EDS analyses suggested that both the core and the rim in Fig. 3b–d were (Ti,M)C solid solutions but the concentration of the heavy alloy elements in the rims was higher than that in the cores. These core-rim structures grains were similar to those found in conventional TiC/Ti(C,N)-based cermets, which are formed by a liquid sintering process. Consequently, the appearance of the blocks with the morphology and microstructure also suggested that a liquid phase
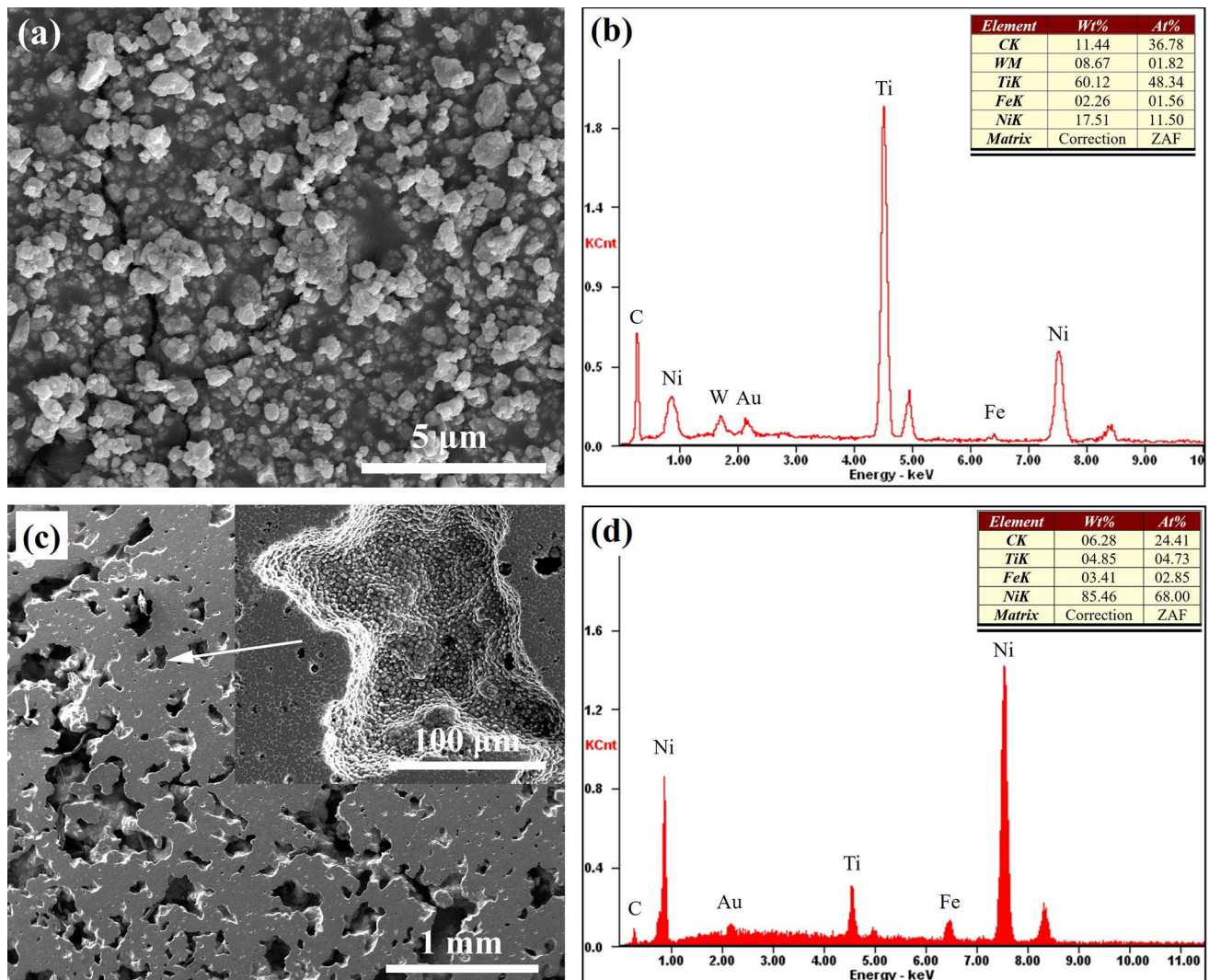

Figure 2 Micrographs of the synthesized composite powder and the block: **a** the ultrafine composite powders; **b** The EDS analysis result of the synthesized TiC-Ni composite powder; **c** the block and its enlarged close-up; **d** The EDS analysis result of the binder phase in the block from Ti-C-Ni system.

Figure 3 SEM-BSE image and EDS analysis of the blocks formed in different systems during MSR: **a** Ti-C-Ni; **b** Ti–W-C-Ni; **c** Ti-Mo-C-Ni; **d** Ti-Ta-C-Ni. The composition of the phases was indicated by elemental atomic ratio.
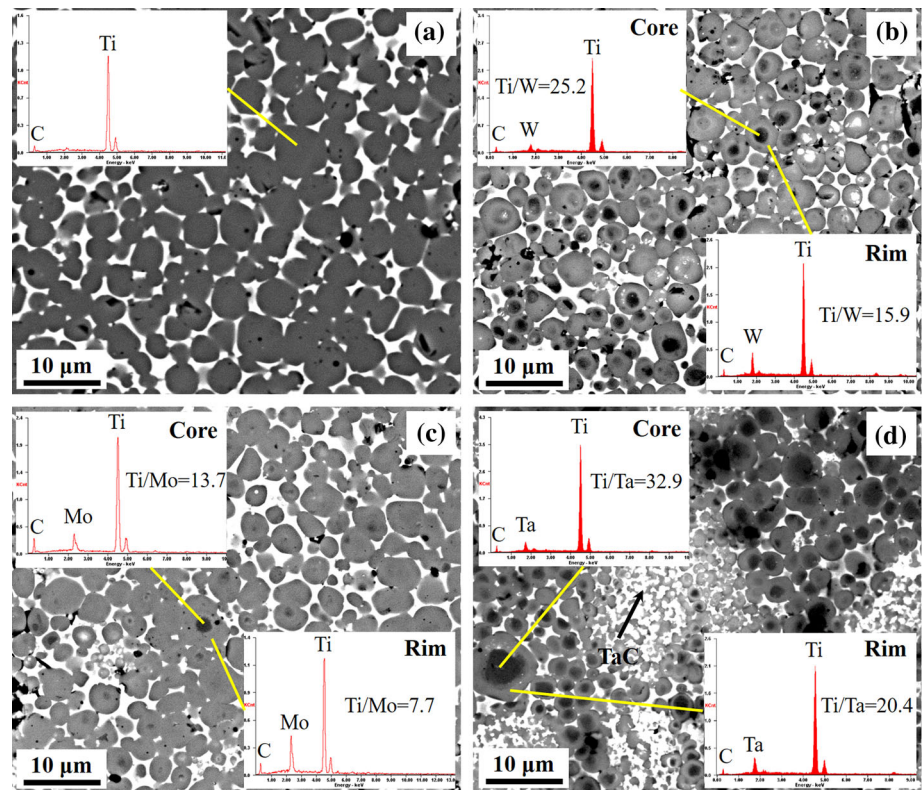
had formed during the MSR [30]. In addition, some TaC particles with very bright contrast due to high atomic number were also included in the Ti-Ta-C-Ni blocks as shown in Fig. 3d, which is consistent with the XRD patterns in Fig. 1. The impurities from the vials were also detected in the synthesized composite powder and blocks by EDS as shown in Fig. 2c, d, and the results indicated only trace amounts of impurities (about 2–3 at.% Fe) remained in the systems.

Microstructure of the cermets

The P1–P4 composite powders after 4 h of ball milling were used to fabricate cermets and were labeled as C1–C4. The phase compositions and microstructures are shown in Figs. 4 and 5, respectively. The XRD patterns indicated that the four kinds of cermets consisted of TiC/(Ti,M)C hard phases and Ni-based binder phases which contained dissolved alloy elements. It also can be observed two types of ceramic grains from the microstructures shown in Fig. 5, one was core-rim structure grain (but without an inner rim) while the other was homogenous (single-phase) grains without a core-rim structure. The phase

composition of the ceramic grains in the microstructures was analyzed by EDS and the results are shown in Table 2. Both the cores and the rims in C2-C4 cermets were (Ti,M)C solid solution but with different Ti/M atomic ratios. This case was similar to the microstructures of the blocks. Obviously, the synthesized (Ti,M)C solid solutions particles acted as the hard phase of the cermets.

The phase composition of the ceramic grains in the cermets (Table 2) suggested that the concentration of the alloy elements in the rims was higher than that in the cores, which was caused by a dissolution and precipitation process. During the liquid-phase sintering, the remnant alloy elements (Ta and W), the secondary carbides TaC and WC (from ball abrasives), and the partial (Ti,M)C solid solution ceramic particles dissolved in the liquid Ni binder and then precipitated in the form of another TiC-based solid solutions on the undissolved (Ti,M)C ceramic particles, forming the rim phases. This is the widely accepted Ostwald ripening mechanism, which has been described as being responsible for the formation of the grains with the core-rim structure in conventional TiC/Ti(C,N)-based cermet systems [10–16]. As shown in Fig. 5c, the (Ti,Mo)C-Ni cermet shows an
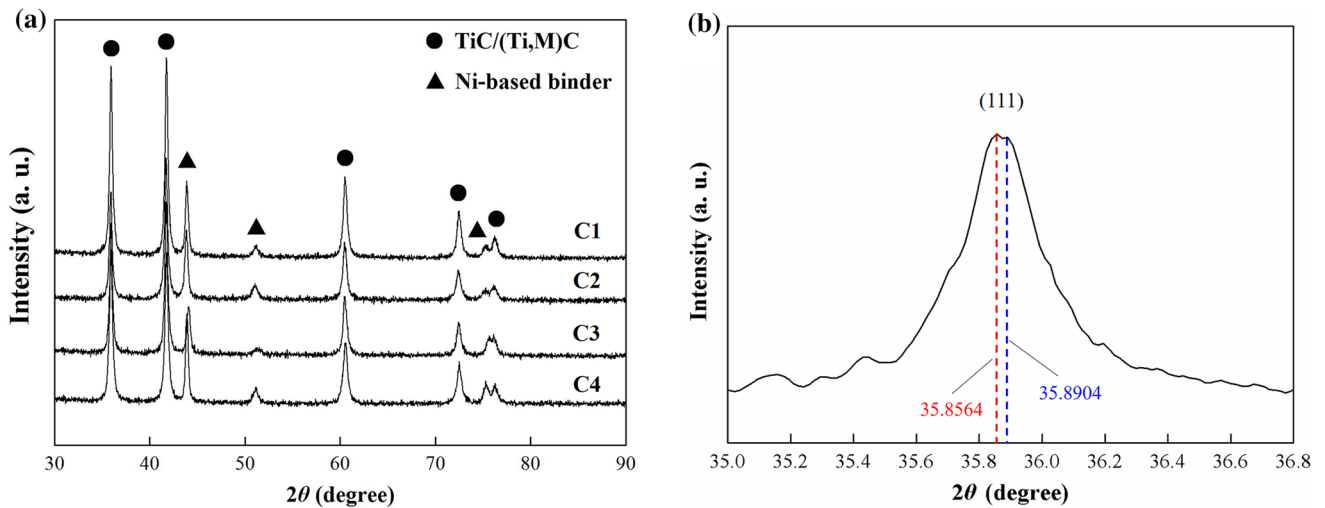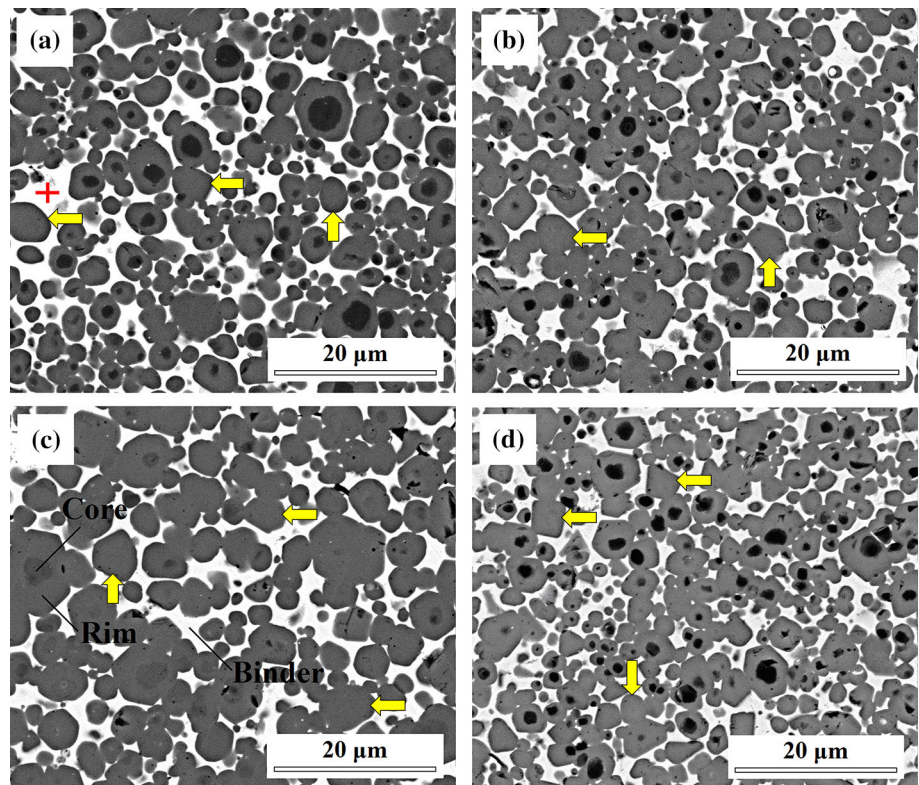
Figure 4 XRD patterns of the cermets: **a** the common patterns of the four kinds of sintered bodies; **b** the local detail of the XRD pattern for C3.

Figure 5 Microstructure of the cermets sintered at 1445 °C for 1 h: **a** TiC-Ni; **b** (Ti,W)C-Ni; **c** (Ti,Mo)C-Ni; **d** (Ti,Ta)C-Ni. The homogenous grains were indicated by yellow arrows.

inconspicuous core-rim structure, which was attributed to the similar composition (Ti/Mo atomic ratio) between the core and the rim (Table 2). However, unlike the formation mechanism of the core-rim structure grains, the single-phase solid solution carbide grains, having a similar composition to the rims, probably precipitated directly from the liquid Ni due to constitutional supercooling, which occurred during the cooling stage of the sintering. Consequently, this kind of ceramic grains lacked the core-rim structure [19].

It's worth noting that the content of the impurities in the binder phase of the sintered cermet was higher than that of the block, as shown in Figs. 3d, 6. This was related to the formation mechanism of the impurities. As the cemented carbides balls are harder

Table 2 Chemical composition of the various phases in the cermets (carbon cannot be accurately quantified by EDS; therefore, only the relative atom fraction of metallic constituents was provided from the average value of five points)

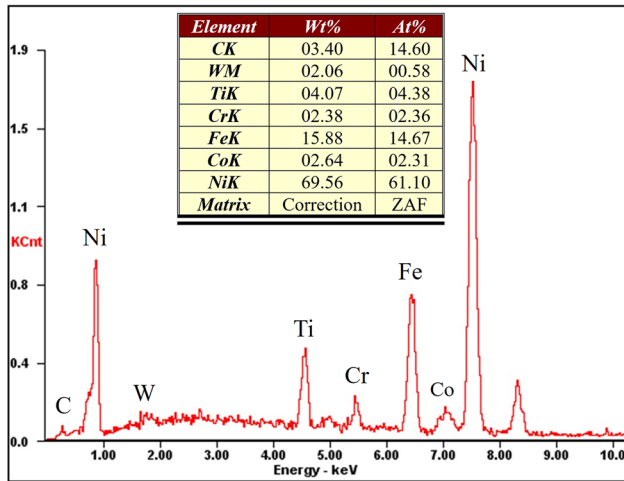| Element	TiC-Ni		(Ti,W)C-Ni		(Ti,Mo)C-Ni		(Ti,Ta)C-Ni	
	Core	Rim	Core	Rim	Core	Rim	Core	Rim
Ti	100	97.30	96.06	90.81	91.76	87.25	96.97	91.11
W	–	2.70	3.94	9.19	–	1.10	–	0.59
Mo	–	–	–	–	8.24	11.65	–	–
Ta	–	–	–	–	–	–	3.03	8.30
Ti/M	–	36.04	24.38	9.88	11.14	7.49	32.00	10.98

Figure 6 The EDS analysis result of the binder phase in the sintered TiC-Ni cermet. The EDS site is indicated by a red cross in Fig. 5a.

than the stainless steel vials, the vials are grinded and scratched by the balls during ball milling collision. Thus, majority of the stainless steel material was adhered on the balls surfaces and only slight stainless steel material mixed into the powders. As a result, the blocks that generated from the mixed powders contained a small amount of stainless steel impurities. In the following process, the composite powders were obtained by several minutes of wet ball milling using alcohol in order to improve the powder yield. Consequently, the adhered stainless steel impurities on the ball surfaces were transferred into the composite powders, which gave rise to the high content of impurities in the sintered cermet. Nevertheless, the high content of the impurities was regarded to be detrimental to the hot hardness and corrosion resistance of the cermets.

Figure 7 shows the HRTEM images of the interfaces in the (Ti,W)C-Ni solid solution cermet. The interface between the binder phase and the ceramic phase was incoherent and had a misorientation angle of 55° (Fig. 7a). Numerous studies have shown that the ceramic phases and binder phases were randomly oriented at their interfaces without a fixed orientation relationship in Ti(C,N)-based cermets [31–34]. The interfaces between the two phases could be coherent or incoherent [35], and this depended on the lattice mismatch between them. From the XRD data and the HRTEM images in Figs. 4 and 7a, the interplanar spacings for (200) plane of the ceramic phase d_1 and (111) plane of the binder phase d_2 were 0.2145 nm and 0.2063 nm, respectively. Thus, the mismatch ($\delta = \frac{d_1 - d_2}{d_1}$) was calculated to be 3.82%, which was large enough to result in the formation of incoherent interface and misorientation. Previous studies also have claimed that there was a slight misorientation between the core and the rim in conventional TiC/Ti(C,N) cermets, which led to the generation of dislocations at the interfaces [31, 35, 36]. However, the interface between the core and the rim in Fig. 7b was coherent due to the remarkably similar compositions, and the lattice mismatch between the core and the rim could be calculated to be 0.09% based on the XRD pattern data shown in Fig. 4b, which suggested a low interfacial stress in the cermets prepared via the mechanochemical technique.

Mechanical properties of the cermets

The porosity and mechanical properties of the (Ti,M)C-Ni solid solution cermets are shown in Table 3. The low porosity of the cermets indicated that the composite powders prepared by MSR were easily sintered to obtain dense bulks by pressureless sintering. The hardness and TRS of the materials were comparable to those of chemically similar, conventionally produced cermets, but the fracture toughness (K_{IC}) of the materials was higher. In particular, the fracture toughness of the (Ti,W)C-Ni cermets was as high as 12.45 MPa m$^{1/2}$. By contrast,

Figure 7 The HRTEM micrographs of the phase boundaries in the (Ti,W)C-Ni cermets: **a** the interface between ceramic phase and binder phase; **b** the interface between the core and the rim.
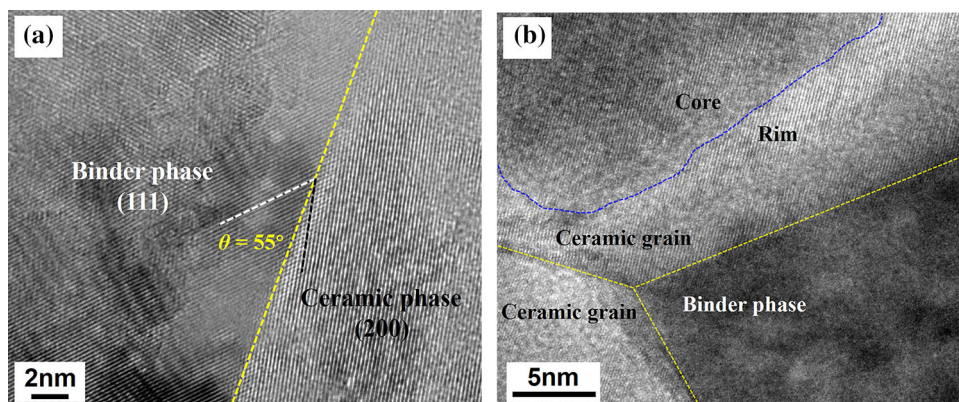

Table 3 Porosity and mechanical properties of the cermets

Cermet	Porosity	Hardness (GPa)	TRS (MPa)	K_{IC} (MPa m$^{1/2}$)
TiC-Ni	A04B00	13.3 ± 0.3	1542.4 ± 49.5	8.28 ± 0.63
(Ti,W)C-Ni	A02B00	14.0 ± 0.2	1644.5 ± 52.5	12.45 ± 0.69
(Ti,Mo)C-Ni	A02B00	13.7 ± 0.2	1581.0 ± 69.0	11.74 ± 0.85
(Ti,Ta)C-Ni	A04B00	14.2 ± 0.2	1559.0 ± 42.0	12.02 ± 0.53

the value of conventional TiC/Ti(C,N)-based cermets is usually less than 10 MPa m$^{1/2}$ [13, 14, 19, 21, 37, 38]. Generally, transgranular fracture was predominant while intergranular fracture was infrequent in conventional TiC/Ti(C,N)-based cermets [18, 20]. However, the two kinds of fracture modes are both observed in Fig. 8 that shows the cracks propagation path of the (Ti,M)C-Ni solid solution cermets caused by Vickers indenter with 30 kg load. The presence of intergranular fracture indicated that cracks propagated in the ductile binder phase, which toughened the cermets by crack bridging and deflection effect.

Discussion

The formation mechanism of the solid solution composite powders

The microstructure of the blocks formed in this study was the same as that of the cermets prepared by Dunmead et al. [39] and Zhang et al. [40] through SHS method. They have confirmed that the spherical TiC grains were formed via the dissolution and precipitation mechanism [39–41]. In this study, the ball milling process of the Ti-C-Ni system can be described as the four stages shown in Fig. 9. At the early stage, all powders are refined and mixed uniformly. The metal powders experienced severe plastic deformation and generated plenty of defects such as

Figure 8 Crack propagation path of the cermets prepared by MSR: **a** (Ti,W)C-Ni; **b** (Ti,Mo)C-Ni. White arrows indicated the trace of intergranular fracture.
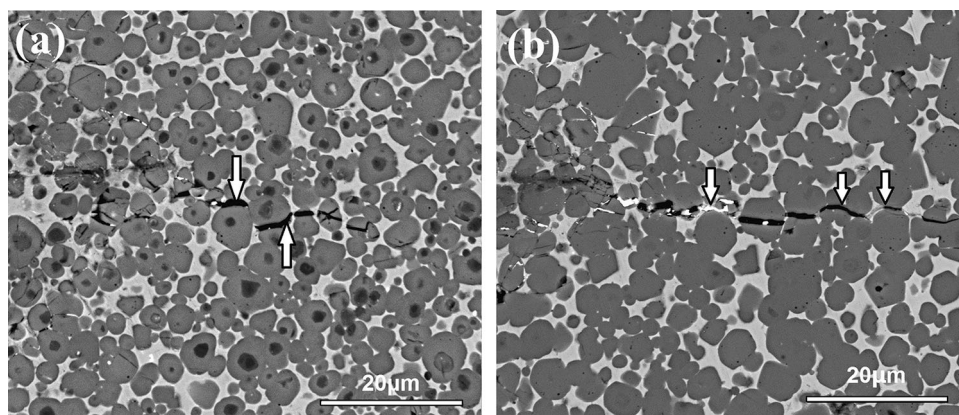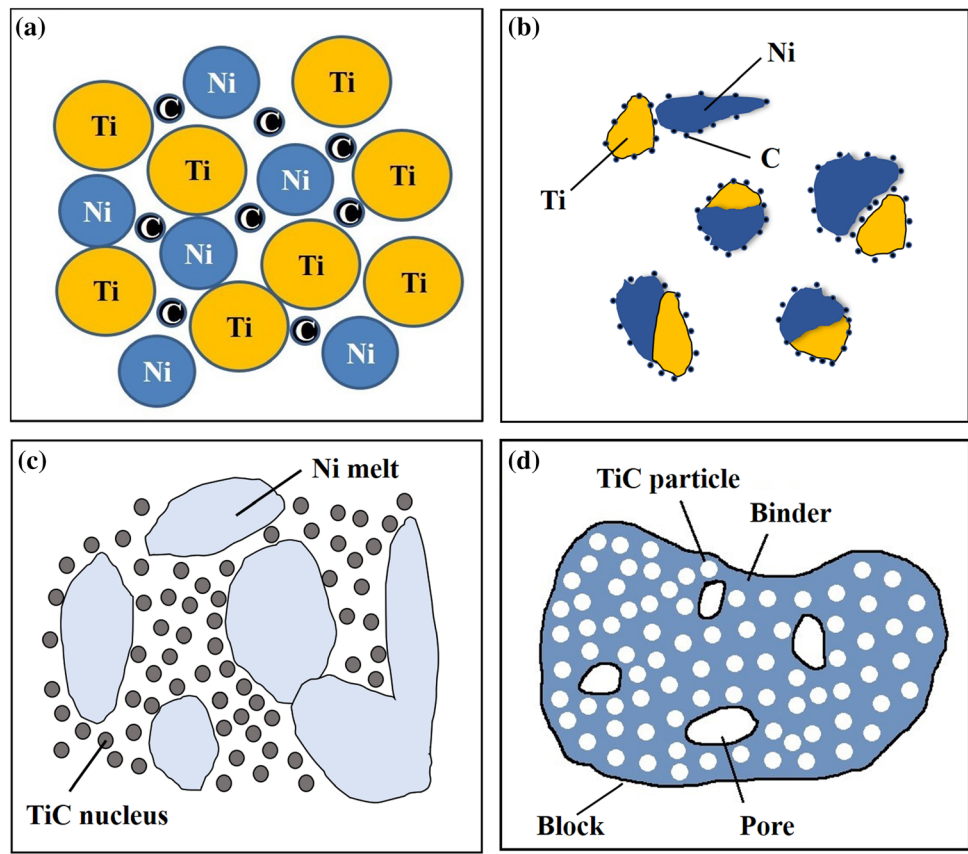
Figure 9 The schematic diagram of Ti-C-Ni system during ball milling. **a** Initial powders are mixed uniformly. **b** The powders were refined and activated. **c** The heat released by the initial formed TiC ignites the combustion reaction and the melts appears. **d** The melts merge and solidify during the cooling stage and form porous block.

vacancies, dislocations and grain boundaries. The refining of the particles also increased the stored strain energy, contact area and activity of the reactants. After a period of the milling, the small graphite fragments attached to the Ti and Ti-inserted Ni powders over lager area. When each particle reached a critical lamellar thickness (fully activated), the reaction between Ti and C was ignited by an instantaneous collision at a certain site and spread quickly through the whole system like the SHS process.

A huge reaction heat raised the temperature abruptly and melted the Ni powders, which acted as the diluent, hindering the MSR and giving rise to a longer activation period. The formation of the liquid phase improved the atoms diffusion rate of the system by dissolving, which promoted a rapid formation and a substantial precipitation of TiC (the spherical particles shown in Fig. 2c). Nevertheless, the released heat lasted a short time and the temperature of the system dropped sharply due to the high frequency of milling balls impact. As a result, the milling balls impacted the solidifying melts which encased TiC grains and divided into many pieces, most of which was refined and became ultrafine composite

powders. However, some melted liquid phase which located at the bottom of the vials were only divided into several large pieces and solidified soon due to the insufficient ball collision at the bottom sites, and eventually became the blocks. Therefore, the ultrafine composite powders were actually the broken form of the blocks.

In the Ti-M-C-Ni systems, the alloying elements W, Mo and Ta were able to dissolve in the liquid phases by means of the large amount of heat released by the MSR (the MSR which occurred in P4 also involved the combustion reaction between Ta and C). Meanwhile, these alloying elements can also diffuse into the newly-formed TiC grains and formed (Ti,M)C solid solution ceramic grains. As the liquid phase solidified, the W, Mo and Ta precipitated in the form of another (Ti,M)C solid solutions on the ceramic grains. Since the dissolution or diffusion rate of the alloy elements in the liquid phase was greater than that in solid phase, the rims exhibited higher concentrations of the alloy element than the cores, leading to a different contrast in the SEM images, i.e., the core-rim structure. Nevertheless, the instantaneous high temperature was responsible for the residual

alloy elements, which resulted in low concentration of alloy elements in (Ti,M)C solid solutions after the MSRs. However, among these alloy elements, Mo was easier to dissolve into the TiC lattice, which also can be confirmed by Mo completely dissolving into TiC through the long ball milling [42, 43]. Consequently, there were inconspicuous core-rim structure grains in the Ti-Mo-C-Ni system.

The toughened mechanism of the cermets

In general, conventional TiC/Ti(C,N)-based cermet systems have a core-inner rim and inner rim-outer rim interfaces besides ceramic grains-Ni binder interface. The interfaces between TiC/Ti(C,N) core and inner rim and outer rim can be highly strained, depending on the composition between these phases. These interfaces are potential sites for crack initiation and propagation [17, 18, 24], which leads to transgranular fracture of the ceramic grains and low fracture toughness in the materials. In the microstructure of the (Ti,M)C-Ni solid solution cermets prepared in this study, however, the core-rim grains did not involve any inner rims and the homogenous grains did not involve any interfaces, thus the interface areas in the cermets reduced significantly. Furthermore, the HRTEM image in Fig. 7b indicated that the stress level of core-rim grains in the (Ti,M)C-Ni solid solution cermets was not as high as that in conventionally produced cermets [18, 35, 36]. In this instance, the transgranular fracture tended to be reduced, while the intergranular fracture increased. Consequently, the (Ti,M)C solid solution exhibited an improved fracture toughness.

On the other hand, the degree of adjacency (namely the contiguity value) of ceramic grains, C_c, was also estimated by using the formula [44–46]

$$C_c = \frac{2N_{cc}}{2N_{cc} + N_{cb}}$$

where N_{cc} and N_{cb} are the average number of intercepts of a line with random direction of unit length with traces of ceramic phase—ceramic phase interfaces and ceramic phase—Ni binder phase interfaces, respectively. The degree of adjacency of ceramic grains was estimated by ImageJ® software based on the SEM micrographs shown in Fig. 5. The contiguity values of ceramic grains for C1–C4 were 0.27, 0.24, 0.32 and 0.23, respectively. Compared to the higher contiguity values (0.35–0.47) in conventional TiC/

Ti(C,N)-based cermets [44–46], the lower degree of adjacency of ceramic grain suggested a well distribution of ceramic grains in binder phase, which is beneficial to crack intergranular propagation and can result in the higher toughness.

Conclusions

TiC-based solid solution cermets were prepared using a mechanochemical method and subsequent pressureless sintering. The ball milling of Ti-M-C-Ni elemental powders triggered a combustion reaction between Ti and C. The heat of reaction promoted the dissolution of alloy elements into the newly formed TiC, which resulted in ultrafine (Ti,M)C-Ni composite powders. The heat released by the combustion reaction also caused a fast liquid sintering process and resulted in the formation of the blocks. There was a misorientation between the ceramic phase and the binder phase, but the interface between the core and the rim was coherent and the stress level of core-rim grains in the (Ti,M)C-Ni solid solution cermets was lower. Consequently, the (Ti,M)C-Ni cermets prepared in this study exhibited mechanical properties that were comparable to conventionally produced cermets, particularly in fracture toughness which was as high as 12.45 MPa m$^{1/2}$.

Author contributions

XC: Experiments Design, Methodology, Writing—Original Draft; ZY: Measurements and Characterization; WX: Reviewing; JX: Writing—Reviewing and Editing

Compliance with ethical standards

Conflict of interest We declare that we have no financial and personal relationships with other

people or organizations that can inappropriately influence our work, there is no professional or other personal interest of any nature or kind in any product, service and/or company that could be construed as influencing the position presented in, or the review of, the manuscript entitled, "A novel fabrication technique of toughened TiC-based solid solution cermets using mechanochemical synthesis".

References

[1] Xu Q, Zhao J, Ai X (2017) Fabrication and cutting performance of Ti(C, N)-based cermet tools used for machining of high-strength steels. Ceram Int 43:6286–6294

[2] Wang H, Gee M, Qiu Q et al (2019) Grain size effect on wear resistance of WC-Co cemented carbides under different tribological conditions. J Mater Sci Technol 35:2435–2446

[3] Akinribide OJ, Obadele BA, Akinwamide SO et al (2019) Sintering of binderless TiN and TiCN-based cermet for toughness applications: processing techniques and mechanical properties: a review. Ceram Int 45:21077–21090

[4] Ishihara S, Goshima T, Nomura K, Yoshimato T (1999) Crack propagation behavior of cermets and cemented carbides under repeated thermal shocks by the improved quench test. J Mater Sci 34:629–636. https://doi.org/10.1023/A: 1004575519293

[5] Fu Z, Kong JH, Gajjala SR, Koc R (2018) Sintering, mechanical, and oxidation properties of TiC-Ni-Mo cermets obtained from ultra-fine TiC powders. J Alloys Compd 751:316–323

[6] Östberg G, Buss K, Christensen M et al (2006) Effect of TaC on plastic deformation of WC–Co and Ti(C, N)–WC–Co. Int J Refract Met Hard Mater 24:145–154

[7] Huang SG, Nie HB, Guo XY (2019) Microstructural investigation and machining performance of NbC-Ti(C0.5N0.5) matrix cermets. Int J Refract Met Hard Mater 84:105038

[8] Rajabi A, Ghazali MJ, Daud AR (2015) Chemical composition, microstructure and sintering temperature modifications on mechanical properties of TiC-based cermet—a review. Mater Des 67:95–106

[9] Lin N, Zhao L, Zou J, Ma C, Wang Z, He Y (2019) Improvement in densification process and properties of Ti (C, N)-based cermets with vanadium carbide addition. Ceram Int 45:2692–2700

[10] Xiong H, Xie D, Chen J et al (2019) Ti(C, N)-based cermets with strengthened interfaces: roles of secondary cubic carbides. J Am Ceram Soc 00:1–11

[11] Lemboub S, Boudebane S, Gotor FJ et al (2018) Core-rim structure formation in TiC-Ni based cermets fabricated by a combined thermal explosion/hot-pressing process. Int J Refract Met Hard Mater 70:84–92

[12] Xiong Z, Ye J, Liu Y, Yang X, Cao Q (2020) Study on the phase evolution, microstructure and densification behavior of (Ti, M)(C, N)-based cermets. Mater Chem Phys 240:122249

[13] Zhou W, Zheng Y, Zhao Y (2018) Study on microstructure and properties of Ti(C, N)-based cermets with dual grain structure. Ceram Int 44(12):14487–14494

[14] Kim ES, Kang S (2001) Precipitation phenomena in MC-Ni-Co cermet systems. J Mater Sci 36:405–410. https://doi.org/10.1023/A:1004876528811

[15] Ahn SY, Kang S (2000) Formation of core/rim structures in Ti(C, N)-WC-Ni cermets via a dissolution and precipitation process. J Am Ceram Soc 83:1489–1494

[16] Kim S, Min K, Kang S (2003) Rim structure in Ti(C0.7N0.3)-WC-Ni cermets. J Am Ceram Soc 86:1761–1766

[17] Park S, Kang S (2005) Toughened ultra-fine (Ti, W)(CN)–Ni cermets. Scrip Mater 52:129–133

[18] Kim J, Seo M, Kang S (2011) Microstructure and mechanical properties of Ti-based solid-solution cermets. Mater Sci Eng A 528:2517–2521

[19] Kim J, Kang S (2011) Microstructure evolution and mechanical properties of (Ti0.93W0.07)C–xWC–20Ni cermets. Mater Sci Eng A 528:3090–3095

[20] Kwon H, Suh CY, Kim W (2015) Preparation of a highly toughened (Ti, W)C-20Ni cermet through in situ formation of solid solution and WC whiskers. Ceram Int 41:4223–4226

[21] Moon A, Suh C, Kwon H (2018) Microstructure and mechanical properties of ultrafine (Ti, Mo, W, Nb, Zr, Ta)(CN)–Ni composites prepared using the stabilized (Ti, Mo, W, Nb, Zr, Ta)(CN) phase. J Alloys Compd 732(25):838–844

[22] Pohan RM, Gwalani B, Lee J et al (2018) Microstructures and mechanical properties of mechanically alloyed and spark plasma sintered Al0.3CoCrFeMnNi high entropy alloy. Mater Chem Phys 210(1):62–70

[23] Bhaskar UK, Pradhan SK (2012) One-step mechanosynthesis of nano structured Ti(CxN1-x) cermets at room temperature and their microstructure characterization. Mater Chem Phys 134(2):1088–1096

[24] Borrell A, Salvador MD, García-Rocha V (2012) Spark plasma sintering of TiyNb1-yCxN1-x monolithic ceramics obtained by mechanically induced self-sustaining reaction. Mater Sci Eng A 543:173–179

[25] Chicardi E, Torres Y, Córdoba JM, Hvizdos P, Gotor FJ (2014) Effect of tantalum content on the microstructure and

mechanical behavior of cermets based on $(Ti_xTa_{1-x})(C_{0.5}N_{0.5})$ solid solutions. Mater Des 53:435–444

[26] Córdoba JM, Chicardi E, Gotor FJ (2012) Development of multicomponent-multiphase materials based on (Ti, Ta, Nb)CxN1-x carbonitride solid solutions. Chem Eng J 192:58–66

[27] Córdoba JM, Sayagués MJ, Alcala MD, Gotor FJ (2007) Monophasic nanostructured powders of niobium, tantalum, and hafnium carbonitrides synthesized by a mechanically induced self-propagating reaction. J Am Ceram Soc 90:381–387

[28] Shetty DK, Wright IG, Mincer PN, Clauer AH (1985) Indentation fracture of WC-Co cermets. J Mater Sci 20:1873–1882. https://doi.org/10.1007/BF00555296

[29] Razavi M, Rahimipour MR, Kaboli R (2008) Synthesis of TiC nanocomposite powder from impure TiO2 and carbon black by mechanically activated sintering. J Alloys Comp 460:694–698

[30] Sheng L, Yang F, Guo J, Xi T, Ye H (2013) Investigation on NiAl–TiC–Al2O3 composite prepared by self-propagation high temperature synthesis with hot extrusion. Compos B Eng 45(1):785–791

[31] Park C, Nam S, Kang S (2016) Carbide/binder interfaces in Ti(CN)–(Ti, W)C/(Ti, W)(CN)-based cermets. J Alloys Comp 657(5):671–677

[32] Yang Q, Xiong W, Zhang G, Huang B (2015) Grain growth in Ti(C, N)-based cermets During liquid-phase sintering. J Am Ceram Soc 98(3):1005–1012

[33] Zhou S, Zhao W, Xiong W, Hong Z (2009) Thermodynamics of the formation of contiguity between ceramic grains and interface structures of Ti(C, N)-based cermets. Int J Refract Met Hard Mater 27(4):740–746

[34] Dong D, Yang W, Xiong H, Zhang L, Shi K, Liao J (2020) Ti (C, N)-based cermets with fine grains and uniformly dispersed binders: Effect of the Ni–Co based binders. Ceram Int 46(2020):6300–6310

[35] Zhang G, Zheng Y, Zhang J, Ke Z, Xu X, Wu H (2020) Interfaces and mechanical properties of dual grain structure Ti(C, N)-based cermets prepared by in situ reduction of TiO2. J Alloys Compd. https://doi.org/10.1016/j.jallcom.2020.154476

[36] Laoui T, Zou H, Van der Biest O (1992) Analytical electron microscopy of the core/rim structure in titanium carbonitride cermets. Int J Refract Met Hard Mater 11:207–212

[37] Mari D, Bolognini S, Feusier G, Cutard T, Viatte T, Benoit W (2003) TiMoCN based cermets. Part II. Microstructure and room temperature mechanical properties. Int J Refract Met Hard Mater 21:47–53

[38] Liu N, Xu Y, Li Z, Chen M, Li G, Zhang L (2003) Influence of molybdenum addition on the microstructure and mechanical properties of TiC-based cermets with nano-TiN modification. Ceram Int 29(8):919–925

[39] Dunmead S, Readey D, Semler C, Birch Hol J (1989) Kinetics of combustion synthesis in the Ti-C and Ti-C-Ni systems. J Am Ceram Soc 72:2318–2324

[40] Zhang XH, Han JC, Du SY, Wood JV (2000) Microstructure and mechanical properties of TiC-Ni functionally graded materials by simultaneous combustion synthesis and compaction. J Mater Sci 35:1925–1930. https://doi.org/10.1023/A:1004714402128

[41] Qi Q, Liu Y, Zhang H (2016) The formation mechanism of TiC particles in TiC/Ni composites fabricated by in situ reactive infiltration. J Mater Sci 51:7038–7045. https://doi.org/10.1007/s10853-016-9994-4

[42] Chen X, Xiong W, Yao Z, Zhang G, Chen S, Yang Q (2014) Characterization of Ti-based solid solution cermets prepared by mechanically induced self-sustained reaction and subsequent pressureless sintering. J Alloys Compd 583:523–529

[43] Kim YK, Shim JH, Cho YW, Yang HS, Park JK (2004) Mechanochemical synthesis of nanocomposite powder for ultrafine (Ti, Mo)C–Ni cermet without core-rim structure. Int J Refract Met Hard Mater 22:193–196

[44] Agnew SR, Keene JI, Dong L, Shamsujjoha M, O'Masta MR, Wadley HNG (2017) Microstructure characterization of large TiC-Mo-Ni cermet tiles. Int J Refract Met Hard Mater 68:84–95

[45] Zhou S, Zhao W, Xiong W (2009) Microstructure and properties of the cermets based on Ti(C, N). Int J Refract Met Hard Mater 27:26–32

[46] Xu X, Ya Z, Zhang G, Ke Z, Ha Wu, Yang Z, Zhou W (2020) Microstructure and mechanical properties of Ti(C, N)-based cermets fabricated using Ni-coated mixed powders. Ceram Int. https://doi.org/10.1016/j.ceramint.2020.03.276